environmental microbiology
environmental microbiology reports

Anaerobic methane oxidation linked to Fe (III) reduction in a Candidatus Methanoperedens-enriched consortium from the cold Zoige wetland at Tibetan Plateau

Journal:	*Environmental Microbiology and Environmental Microbiology Reports*
Manuscript ID	EMI-2021-1605.R1
Journal:	Environmental Microbiology
Manuscript Type:	EMI - Research article
Date Submitted by the Author:	10-Nov-2021
Complete List of Authors:	Chen, Lin Li, Lingyan Zhang, Shengjie Zhang, Wenting Xue, Kai; University of Chinese Academy of Sciences, College of Resource and Environment Wang, Yanfen; Chengdu Institute of Biology, Key Laboratory of Mountain Ecological Restoration and Bioresource Utilization & Ecological Restoration Biodiversity Conservation Key Laboratory of Sichuan Province Dong, Xiuzhu
Keywords:	Anaerobic oxidation of methane, Fe (III) reduction, Ca. Methanoperedens psychrophilus, unique genes in cold adaptability, Zoige wetland

Anaerobic methane oxidation linked to Fe (III) reduction in a *Candidatus Methanoperedens*-enriched consortium from the cold Zoige wetland at Tibetan Plateau

Lin Chen[1#], Lingyan Li[1,2#], Shengjie Zhang[1,2], Wenting Zhang[1,2], Kai Xue[1], Yanfen Wang[1*], Xiuzhu Dong [1,2*]

1, University of Chinese Academy of Sciences, No.19A Yuquan Road, Shijingshan District, Beijing 100049, China

2, State Key Laboratory of Microbial Resources, Institute of Microbiology, Chinese Academy of Sciences, Beijing 100101, PR China

Correspondence to: Xiuzhu Dong, No.1 Beichen West Road, Beijing 100101. Tel. 86-10-64807413, Email: dongxz@im.ac.cn; and Yanfen Wang, Email: yfwang@ucas.ac.cn

#, these authors contributed equally

Originality-Significance Statement

Anaerobic oxidation of methane (AOM) is a microbial process that consumes large portion of methane, and *Candidatus Methanoperedens* implemented nitrate-reduction coupled AOM is frequently found in mesophilic freshwater systems (22°C to 35°C). This work for the first-time reports that Fe (III)-, but not nitrate-reduction linked AOM is active in a cold wetland at Tibetan Plateau, which appears occurring only at lower temperatures like 18°C, but not 30°C. The cold active AOM is implemented by a cold adaptive *Ca. Methanoperedens* population, which represents a novel species *Ca. Methanoperedens psychrophilus*. Comparative genomic analysis revealed the unique genes of *Ca. Methanoperedens psychrophilus* that may be related to its cold adaptability, like the S-layer proteins and type IV pili.

Summary

Anaerobic oxidation of methane (AOM) is a microbial process degrading ample methane in anoxic environments, and *Ca. Methanoperedens* mediated nitrate- or metal-reduction linked AOM is believed important in fresh water systems. This work, via 16S rRNA gene diversity survey and 16S rRNA quantification, found abundant *Ca. Methanoperedens* along with iron in the cold Zoige wetland at Tibetan Plateau. The wetland soil microcosm performed Fe(III) reduction, rather than nitrate- nor sulfate-reduction, coupled methane oxidation (3.87 μmol·d^{-1}) with 32.33 μmol Fe(II) accumulation per day at 18°C, but not at 30°C. A metagenome-assembled genome

(MAG) recovered from the microcosm exhibits ~74% average nucleotide identity with the reported *Ca. Methanoperedens* spp. that perform Fe(III) reduction linked AOM, thus a novel species *Ca. Methanoperedens psychrophilus* was proposed. *Ca. M. psychrophilus* contains the whole suite of CO_2 reductive methanogenic genes presumably involving in AOM via a reverse direction, and comparative genome analysis revealed its unique gene categories: the multi-heme clusters (MHCs) cytochromes, the S-layer proteins highly homologous to those recovered from lower temperature environments and type IV pili, those could confer *Ca. M. psychrophilus* of cold adaptability. Therefore, this work reports the first methanotroph implementing AOM in an alpine wetland.

Introduction

Methane (CH_4) is the second abundant greenhouse gas following carbon dioxide, and contributes about 20% to the current global warming (He et al., 2018). Whereas, both aerobic and anaerobic oxidations of methane (AOM) have consumed large portion of methane, by proximately 90% of the marine (Ding et al., 2016) and 50% fresh water CH_4 (Segarra et al., 2015).

AOM is a microbial process implemented by a specific group of methanotrophic archaea that oxidizes CH_4 using different electron acceptors except oxygen in various ecosystems (Gupta et al., 2013; McGlynn et al., 2015; Timmers et al., 2016). Sulfate reduction coupled AOM was firstly reported in marine by the syntrophism of anaerobic methanotrophic archaea (ANMEs) and sulfate-reducing bacteria (SRB) (Wegener et al., 2015). Later, nitrate reduction coupled AOM by the consortium of *Candidatus Methanoperedens nitroreducens* and *Methylomirabilis oxyfera* is described in fresh water (Haroon et al., 2013).

Iron is the second richest metal species in the earth's crust, and Fe(III) reduction linked methane oxidation is a chemical reaction with favorable thermodynamics comparing with that coupled to sulfate reduction (Bonneville et al., 2009). Therefore, Fe(III) reduction-AOM is assumed to be widely distributed. Indeed, Fe(III) or Mn(IV)-dissimilatory reduction, rather than of nitrate, linked AOMs have been reported recently, and a novel *Ca.* genus of *Methanoperedens* implements the processes (Ettwig et al., 2016; Cai et al., 2018; Leu et al., 2020). Moreover, the *Ca. Methanoperedens* methanotrophs that affiliate with ANME-2d are frequently found in freshwater systems

and reservoirs (Hu et al., 2009; Meulepas et al., 2009), and the mesophilic (22°C to 35°C) enrichments containing *Ca. Methanoperedens* have been obtained (Ettwig et al., 2016; Cai et al., 2018; Leu et al., 2020). Therefore, *Ca. Methanoperedens* could represent the major non-marine ANMEs, whereas, no purified culture has been obtained up to date.

The cold Zoige wetland is at 3400 to 3600 m above sea level (asl) and under the average annual temperatures from −1.7 to 3.3℃; while it is one of methane emission centers of Tibetan plateau (Jin et al., 1999), suggesting that abundant cold-active methanogens could inhabit in the Zoige wetland. We did find a dominant uncultured methanogen cluster ZC-I in this wetland when surveyed the archaea diversity (Zhang et al., 2008a; Zhang et al., 2008b), which exhibits higher 16S rRNA similarity to that of *Ca. Methanoperedens nitroreducens* BLZ1 that has been enriched from Fe(III) fed reactors (Ettwig et al., 2016). This suggests that the ZC-I cluster methanogens could also implement AOM coupled to Fe(III) reduction. Iron was found as the second most abundant metal element in Zoige wetland (Wang et al., 2017), but nitrate was at lower levels (Zhou et al., 2019; Xie et al., 2020). Therefore, Fe(III)-reduction coupled AOM could be active in this cold alpine wetland.

To explore whether AOM occurs and what the dominant AOM pathways present in the cold Zoige wetland, in this study, we first surveyed the archaea diversity, and found multiple methanogenic archaea families along with the *Ca. Methanoperedens* population that may be active in the wetland soil based on the 16S rRNA abundance. A microcosm that performed Fe(III) reduction coupled AOM at 18°C but not at 30°C was

obtained, from which the metagenome assembled genome (MAG) of a *Ca. Methanoperedens* representative was obtained. Comparative genome analysis revealed the distinct genes of the cold wetland *Ca. Methanoperedens* MAG from the reported relatives. Therefore, this work reports a cold adaptive *Ca. Methanoperedens* that implements AOM specifically coupled to Fe(III) reduction in the cold Zoige wetland.

Results and discussion

The *Ca. Methanoperedens* population is distributed in the cold Zoige wetland

To probe whether the anaerobic methanotrophs (ANMEs) inhabit in the cold Zoige wetland, we surveyed the archaea diversities in three sites, Hong-yuan (HY, 0 − 40 cm in depth), Ruo-er-gai (RG, 0 − 20 cm in depth) and Hua-hu (HH, 0 − 20 cm in depth), and the geographic locations are shown in Figure 1a.

Upon amplifying and sequencing the archaeal 16S RNA genes retrieved from the three wetland soils, the archaeal diversity and the relative abundances of each phylogenetic group were evaluated based on 16S rRNA homology and read coverages. As shown in Figure 1b, Methanobacteriaceae, Rice cluster Ⅱ and *Ca.* Methanoperedenaceae were present as top 3 of relative abundances among the detected archaea in the three sampling sites. In total, 476 OTUs were assigned to the *Ca.* genus *Methanoperedens*.

Next, the phylogenetic relationship of *Ca. Methanoperedens* in Zoige wetland with those from other environments was analyzed based on the 16S rRNA gene sequence in length of approximate 1 Kb. In total, 210 16S rRNA gene sequences were obtained and

phylogenetic analysis determined that the *Ca. Methanoperedens* population in Zoige wetland could possess eleven phylogenetic clades (Fig. 1c). Ten of the eleven Zoige clades comprising of 94% 16S rRNA clones exhibited 91.1% − 99.3% sequence similarities with the *Ca. Methanoperedens* from low temperatures (15 − 18℃) fresh water systems, like Xiang-jiang and Jiu-long-jiang rivers. Only 6% Zoige *Ca. Methanoperedens* were clustered with those from the higher temperature environments like mud volcano and hydrothermal vent. This suggests that Zoige wetland may harbor predominantly cold adaptive *Ca. Methanoperedens* population.

The *Ca. Methanoperedens* population appears active in one wetland soil containing rich methane and iron

To explore whether *Ca. Methanoperedens* implements AOM in the cold Zoige wetland, the HY soil, in which abundant *Ca.* Methanoperedenaceae was detected (Fig.1b), was chosen for further study. Methane, the AOM substrate, released from the soil samples was first assayed. By dissolved the different soil layers from 0 − 40 cm in depth in pre-reduced distilled water within anaerobic serum bottles, methane was determined from all the soil slurries after 70 day-incubation at 18℃ (Fig. 2a), by the upper layers of 0 −10 cm in depth having the highest CH_4 release rate, and the deeper of the soil layer, the lower of the CH_4 producing rate. This indicates that rich methane is produced in the upper soil layers. Next, the known electron acceptors used in AOM were assayed in the soil samples. As shown in Figure 2b, iron is the most abundant element in each soil layer, and followed by dissolved organic carbon (DOC) and manganese, whereas only low amounts of sulfate and nitrate were measured in all the

soil layers.

Next, the abundance of the *Ca. Methanoperedens* population in HY soil was assessed based on quantification of the 16S rRNA gene copies. By using the *Ca. Methanoperedens nitroreducens* specific 16S rRNA primers, most abundant 16S rRNA gene of *Ca. Methanoperedens* was detected in the soil layers of 20 − 40 cm in depth (Fig. 2c), which made up 11% − 14% of total archaea, while only 0.6% in the layer of 0 − 5 cm. Although higher abundance of the *Ca. Methanoperedens nitroreducens* 16S rRNA gene in deeper soil (>30 cm in depth) was reported in Hua-Hu lake, another site of the Zoige wetland (Xie et al., 2020), the assessed distribution of this methanotroph is inconsistent with that of methane production, its substrate, mainly in the upper soil layer (Fig. 2a). Hence, we further quantified the 16S rRNA copies of *Ca. Methanoperedens* population in the same soil layers using reverse transcription quantitative PCR. In contrary to the assessment on 16S rRNA gene, the highest *Ca. Methanoperedens* 16S rRNA copies were detected in the soil layer of 0 − 5 cm in depth, by accounting for ~3% of total archaea, but 1.4% in the layer of 20 – 40 cm (Fig. 2d). This indicates that the *Ca. Methanoperedens* population can be most active in the methane rich soil layer.

A lower temperature enrichment implementing Fe(III) reduction coupled CH_4 oxidation is obtained from the Zoige wetland

To experimentally verify AOM process present in the cold Zoige wetland, the wetland soil sampled from HY site was used as the inoculant to enrich the *Ca. Methanoperedens* archaea in a pre-reduced mineral medium (Vaksmaa et al., 2017).

Methane gas was fed and electron acceptors either of ferric citrate (pH=6.8), or nitrate or sulfate was amended, and ampicillin and kanamycin were also added to suppress the soil bacteria. The enrichments were incubated at 18°C or 30°C. Until 95-day incubation, methane degradation was only found in Fe(III) amended enrichment at 18°C, but not in other or non-electron acceptor amended cultures (Fig. 3a). Following, 20 mM ferric citrate was amended in a two-week interval into the enrichment and continued the incubation at 18°C till 155 days, and the methane consumption at a rate of 3.87 μmol·d^{-1} and Fe(II) accumulation rate of 32.33 μmol·d^{-1} were determined, respectively (Fig. 3b). Thus, an 8.25:1 molecular ratio of Fe(II) accumulation to methane consumption roughly conforms the stoichiometry of Fe(III) reduction coupled AOM (Ettwig et al., 2016; Cai et al., 2018). Comparing with the AOM rate, 16.69 μmol CH_4·d^{-1}, of a mesophilic enrichment of an Australia reservoir sediment, in which *Ca. M. ferrireducens* was enriched (Cai et al., 2018), AOM in the cold Zoige wetland has a marked lower methane degradation rate. To further verify the Fe(III) reduction coupled methane oxidation produced CO_2, ^{13}carbon labeled CH_4 was amended to the soil enrichment at day 110 of the incubation at 18°C. Using an isotope ratio gas mass spectrometer, similar rates of $^{13}CH_4$ decrease and $^{13}CO_2$ increase were assayed in the Fe (III) reduction-coupled AOM enrichment (Fig. 3c), thus confirms the AOM in Fe(III) amended soil enrichment. However, neither methane degradation (Fig. S1a) nor $^{13}CO_2$ production (Fig. S1b) was detected in Fe(III) amended enrichment at 30 ° C until 160-day incubation. This indicates that the cold Zoige wetland could only harbor the cold adaptive AOM methanotrophic archaea.

188 To link the *Ca. Methanoperedens* activity with the measured methane degradation
189 in the enrichments, changes of the *Ca. Methanoperedens* specific 16S rRNA gene
190 abundance were followed using quantitative PCR during incubation. It found that the
191 *Ca. Methanoperedens* 16S rRNA gene copies were increased from 32.3 at day 41 to
192 812.3 copies·ng^{-1} community DNA at day 153 (Fig. 4d), an indicative of *Ca.*
193 *Methanoperedens* being highly enriched, therefore, they should be the major player in
194 Fe(III) reduction coupled AOM of the wetland. The possibility of bacteria involving in
195 Fe(III) reduction and aerobic methane oxidation was excluded because of a continuous
196 amendment of antibiotics.

197 **Phylogenomic analysis suggests the *Ca. Methanoperedens* population in Zoige**
198 **wetland representing a novel species**

199 To obtain insights into the genetic characteristics of the cold active *Ca.*
200 *Methanoperedens* enriched from the Zoige wetland, the Fe(III) reduction coupled AOM
201 enrichment at day 153-incubation was used for metagenomic analysis. In total, 242 Gb
202 DNA sequences were obtained and binned to the population genomes, and three
203 completed *Ca. Methanoperedens* genomes (completeness > 50%, contamination<10%)
204 (Dataset S1) were recovered, in which Fe_bin.173 is the most completed one with 98.03%
205 completeness and 2.6% contamination.

206 A phylogenomic tree constructed using the concatenated 122 archaeal marker
207 proteins confirmed the phylogenetic placement of the three *Ca. Methanoperedens*
208 MAGs within the *Candidatus* family of Methanoperedenaceae, but they grouped as an
209 independent branch at the highest sequence identity of ~ 70% with the other *Ca. M.*

nitroreducens species (Fig. 4). In addition, the Fe_bin.173 MAG, a representative wetland *Ca. Methanoperedens,* exhibits only 73.7 − 74.8% average nucleotide identities (gANI) and 72.7 − 73.3% amino acid identity (gAAI) with the four available *Ca.* Methanoperedenaceae genomes, *Methanoperedens nitroreducens, Methanoperedens nitroreducens* BLZ1, *Methanoperedens manganicus,* and *Methanoperedens ferrireducens*, those were all recovered from bioreactor enrichments. Therefore, combined with the relative lower gAAI and relative distant phylogenomic relationship with the described *Ca. Methanoperedens* spp., the three *Ca. Methanoperedens* recovered from the cold Zoige wetland could represent a new species, for which *Ca. Methanoperedens psychrophilus* nov. sp. was proposed.

Metabolic construction of the putative Fe(III) reduction coupled AOM pathway in *Ca. Methanoperedens psychrophilus*

To get an insight into the putative AOM metabolic pathway of *Ca. M. psychrophilus*, the assembled metagenome of Fe_bin.173 (GenBank acc. JAGFND000000000) was analyzed. MAG Fe_bin.173 is in length of 2.78 Mbp, which was assembled from 27 scaffolds, and encodes 3,094 ORFs and 33 annotated tRNAs. Resembling the reported *Ca. Methanoperedens* MAGs, Fe_bin.173 carries all the genes involved in CO_2 reductive methanogenesis pathway (Dataset S1), and those encoding electron transfer proteins or complexes, like the Fpo complex and both the membrane associated and cytoplasmic heterodisulfide reductase complexes, HdrDE and HdrABC, in addition of the methanogen specific cofactors such as coenzyme M and B (Fig. 5a). Thus, methane oxidation through the "reverse methanogenesis" pathway is predicted by *Ca. M.*

232 *psychrophilus* Fe_bin.173 as well.

233 Similar to *Ca. M. ferrireducens*, Fe_bin.173 does not possess *narGH* for nitrate
234 reductase complex and was incapable of nitrate reduction coupled AOM; whereas both
235 *Ca. M. nitroreducens* BLZ1 (Ettwig et al., 2016) and *M. nitroreducens* (Haroon et al.,
236 2013) carry *narGH* and implement AOM coupled to nitrate reduction. However, as
237 other Methanoperedenaceae members, which encode a diverse repertoire of multi-heme
238 c-type cytochromes (MHCs, ≥ three CXXCH motifs), Fe_bin.173 MAG encodes 15
239 MHCs that contain 77 CXXCH motifs (Dataset S1). In addition, one putative
240 MK:cytochrome *c* oxidoreductase gene cluster was identified, including two
241 cytochrome *b*-561 (PPOFJMJL_00895, PPOFJMJL_00896) and two 6-heme c-type
242 cytochromes (PPOFJMJL_00890, PPOFJMJL_00891). MHCs have been suggested to
243 facilitate electron transfer from MK re-oxidation to metal oxides or direct interspecies
244 electron transfer (DIET) between syntrophic partners (Kletzin et al., 2015; Ettwig et al.,
245 2016; Cai et al., 2018). Bioinformatic analysis indicated that the MHC containing
246 proteins in Fe_bin.173 are falling into three categories: the NrfA-NrfH like protein
247 complexes, the extracellular S-layer architecture, and class III cytochrome C family
248 (Dataset S1). Cytochrome *b, c* and Nrf complexes are frequently found in other metal-
249 reducing microorganisms that mediate electron transport from cytoplasm to periplasm
250 (Leu et al., 2020). Fe_bin.173 also contains genes encoding membrane associated
251 cytochrome *c*/nitrite reductase complex NrfA/NrfB or NrfA/NrfH, different from NrfD
252 in *Ca. M. ferrireducens*. Proteins with MHC/S-layer fusion were assumed to mediate
253 electron transfer across the S-layer protein of marine ANME-2 (McGlynn et al., 2015),

and they were relatively higher expressed in *Ca. M. manganicus* and *Ca. M. manganireducens* when coupled AOM to Mn (IV) reduction (Leu et al., 2020). Conversely, the *Ca. M. ferrireducens* MHC/S-layer genes were not unregulated during Fe(III) reduction coupled AOM (Cai et al., 2018), thus no indicative of the MHC/S-layer proteins involving in Fe(III) but presumably Mn(IV) reduction coupled AOM. Therefore, the three categories of MHC containing proteins, NrfA-NrfH like protein complexes, the extracellular S-layer architecture and class III cytochrome C family, are assumed to mediate electron export during methane oxidation by *Ca. M. psychrophilus*.

Comparative genome analysis reveals the distinct gene categories of *Ca. M. psychrophilus* from other *Methanoperedens* members

Through comparative genome analysis against the four available Methanoperedenaceae genomes recovered from Fe- and Mn-reducing AOM enrichments, 525 unique genes were identified in *Ca. M. psychrophilus* (Fig. 5b). Of these, seven encoding cell surface proteins and six encoding glycosyl transferase have been identified, this suggests that *Ca. M. psychrophilus* may adopt some genes involved in remodeling the cell envelope in response to cold. These proteins all possess an N-terminal signal peptide that are predicted to be secreted via the Sec dependent pathway or anchored via a C-terminal membrane anchor. Among those, PPOFJMJL_00201 encodes COG1361 S-layer domain by 61.3% and 56.8% amino acid homologies respectively to those of *M.* HGW-Methanoperedenaceae-1 and ANME-2a, the two MAGs were enriched from cold groundwater and cold seep, respectively (Hernsdorf et al., 2017; Yang et al., 2020). PPOFJMJL_00202, a gene adjacent to the COG1361 S-

layer domain encodes a MacB-like periplasmic core domain, by exhibiting a high similarity with *M.*HGW-Methanoperedenaceae-1 and ANME-2a. Type IV pili have been reported to play important roles in surface adhesion and twitching motility. PPOFJMJL_01811 encodes a protein at a high amino acid sequence similarity with the *Methanococcoides* and *Methanosarcina* type IV pili, which could exert roles in facilitating cell clump formation when grown at low temperatures (Saunders et al., 2006). Therefore, the COG1361 S-layer domain and type IV pili could be related to the cold adaptation of the wetland *Ca. Methanoperedens psychrophilus.* PPOFJMJL_01139 encodes a dolichyl-phosphate-mannose-protein mannosyltransferases, which together with other five glycosyl transferases (PPOFJMJL_00541, PPOFJMJL_00540, PPOFJMJL_00817, PPOFJMJL_02010 and PPOFJMJL_01139) could involve in N-glycosylation of the cell surface proteins, a type of post-translation modification of proteins occurs when organisms are under stresses (Eichler, 2020; Li et al., 2020).

Remarkably, the virulence-associated protein (Vap) toxin-antitoxin (TA) locus was also found in the unique gene category of the *Ca. M. psychrophilus* MAG, in which *vapB* encodes the proteolytically labile antitoxin (Lu et al., 2016) and *vapC* encodes a stable ribonucleolytic toxin VapC. In addition, *Ca. M. psychrophilus* also carries the genes for MazE, a bacterial antitoxin, and an archaeal toxin gene. VapBC is the most abundant TA loci family in extreme thermoacidophiles, such as *Sulfolobus tokodaii* and *Sulfolobus solfataricus* (Cooper et al., 2009). The pA3J1 plasmid from the psychrotolerant Antarctic *Pseudomonas* sp. ANT_J3 carries a toxin-antitoxin system

(Relbe homologue), and that was predicted playing roles in cold adaptation (Romaniuk et al., 2017). Therefore, the *Ca. M. psychrophilus* VapBC TA system could involve in its cold adaptation as well.

Interestingly, in comparison with the other *Methanoperedens* members, the gas vesicle encoding gene cluster *gvpF-gvpO-gvpN-gvpA* was observed in the *Ca. M. psychrophilus* MAG. Gas vesicle is only found in *Halobacterium* (Shukla and DasSarma, 2004), which could facilitate haloarchaea rising to water surface. We hypothesized that *Ca. M. psychrophilus* could make use of the gas vesicles to store methane.

In conclusion, this work reports a Fe (III)-, but not nitrate-reduction linked AOM process in a cold wetland at Tibetan Plateau, and the process is implemented by a cold adaptive *Ca. Methanoperedens* population. Based on the lower (~74%) average nucleotide identity of the MAG recovered from the wetland microcosm with reported *Ca. Methanoperedens*, and they implemented AOM only at lower temperatures but not at 30 °C, a novel species, *Ca. Methanoperedens psychrophilus,* is proposed for the population. Comparative genome analysis did find the unique genes that may be related to the cold adaptability of *Ca. M. psychrophilus*. Therefore, this work for the first time reports a methanotroph implementing AOM in an alpine wetland.

Experimental procedures

Wetland soil sample collection

Wetland soils were sampled from three sites: Hua-hu wetland park (HY), Ruo-er-gai County (RG) and Hong-yuan County (HY), of the Zoige wetland at Tibetan Plateau,

located in the region at 33°56′N, 102°52′E (Figure 1a) in June of 2019. Soil samples were collected in anaerobic bio-bag and stored in dry ice during transportation to laboratory. Each sample was divided into two aliquots by one stored under 4℃ for chemical analysis and the other frozen at −80℃.

Soil chemicals analysis

Soil NO_3^- was extracted with 2 M KCl and determined using Ion Chromatography (Alliance, France); and soil SO_4^{2-} was extracted using $Ca(H_2PO_4)_2$ and determined using $BaSO_4$ turbidimetric method (Ajwa and Tabatabai, 1993). Total dissolved organic carbon (DOC) was determined using a TOC Analyzer (TOC-Vcph, Shimadzu, Japan). Total iron (Fe) and manganese (Mn) were measured using quadrupole inductively coupled plasma mass spectroscopy (ICP-MS, Thermo Elemental, X-Series); while soluble iron in pore water was measured spectrophotometrically using phenanthroline under anaerobic condition (Shi et al., 2020).

Measurement of methane

The soil sample (0.5 g) was dissolved in 5 mL pre-reduced distilled water within anaerobic serum bottles, and incubated under 0.1 MPa N_2 gas at 18°C. 40 μL gas was sampled using a syringe with air switch for methane measurement by GC-14B gas chromatograph (Shimadzu), which is equipped with a flame ionization detector and a C18 column as described previously (Zhang et al., 2004), and the temperature parameters as follows: column temperature at 50°C, injector temperature at 80°C, and detector temperature at 130°C.

Anaerobic methane oxidation enrichment using various electron acceptors

Soil sample (5 g) was dissolved in 50 mL pre-reduced mineral medium prepared as described previously (Vaksmaa et al., 2017) within a 100 mL-anaerobic serum bottle under 0.1 Mpa of methane (99.99%), and incubated at 18℃. After two weeks incubation until the potential electron acceptors, Fe^{3+}, NO_3^-, SO_4^{2-}, for AOM in the soil samples depleted to the detection limitation, a final concentration of 20 mM of ferric citrate (pH=6.8), sodium nitrate and sodium sulfate were each pulse-fed to the enrichment culture every two weeks. Meanwhile, a final concentration of each 100 mM of ampicillin and kanamycin was amended every two weeks to inhibit bacteria. An enrichment without electron acceptor amended was included as a control. The enrichments in four replicates were continuingly incubated at 18℃ or 30℃ under gently shaking at 80 rpm. Methane degradation and the amended electron acceptors were measured every 10 days during the 160 day-incubation.

Mass- and electron-balance calculation

Profiles of methane and Fe (II) contents in above enrichments from day 110 till day 160 of incubation were used to determine the methane consumption rate (rCH_4) and Fe (II) accumulation rate (rFe (II)) via a linear regression to evaluate the Fe (III) contribution to AOM. Measurements from at least triplicate cultures were used for the calculations.

Carbon isotopic labelling tests

Three AOM enrichments amended with ferric citrate above were added with approximately 80 μL ^{13}C-labelled methane (Sigma-Aldrich, 99 atoms % ^{13}C, USA) at day 110 of the incubation. $^{13}CH_4$ and $^{13}CO_2$ were determined using an Isotope ratio

mass spectrometry (Thermo Fisher, USA), and changes of the carbon isotopic fractions were used to evaluate anaerobic oxidation of methane.

DNA and RNA extraction

DNA was extracted from ~ 0.5g of the soil samples and ~2 mL enrichment cultures using the MoBio Power soil DNA Isolation Kit (MoBio, Carlsbad, CA, United States) according to the manufacturer's protocol. RNA was extracted from the HY soil (~0.5 g) using RNeasy PowerSoil (QIAGEN) Total RNA Kit. Purified DNA and RNA were quantified using NanoDropND-100 Spectrophotometer (Gene Company), and the qualities of extracted RNA and DNA were examined by 1% agarose gel electrophoresis.

Illumina sequencing of the soil archaeal 16S rRNA genes

The archaeal 16S rRNA diversity in the wetland soils were surveyed via High throughout sequencing. Primers Arch519F and Arch915R were used to amplify a 399-bp fragment of the archaeal 16S rRNA gene flanking the V4 and V5 regions. Purified amplicons were sequenced by Novogene company (Beijing, China) and processed the Illumina Miseq sequencing with standard protocols and the data using QIIME (version 1.7.0) pipeline (Caporaso et al., 2010). Operational taxonomic units (OTU) tables were generated from the pipeline.

PCR amplification and clone library construction of the Methanoperedeneceae specific 16S rRNA gene

The Methanoperedeneceae specific 16S rRNA gene was amplified using a modified primer set of 109F/1115R (Narihiro and Sekiguchi, 2011) (Table S1) to amplify a 1007-bp fragment. PCR amplification is performed as 94 °C for 5 min, followed by 30

cycles consisting of 94 °C for 30 s, 52 °C for 30 s, 72 °C for 40 s, and a final extension period of 72 °C for 10 min. The fragments were purified using the Gene JET PCR purification kit according to the manufacturer's protocol. The amplified PCR products were cloned into the pMD19-T vector and transformed to *E. coli* DH5α. The positive transformants were sequenced at BioSune Biotechnology (shanghai) Co., Ltd.

Quantitative real-time PCR and reverse transcription quantitative (RT)-PCR

Quantitative qPCR reactions were performed in eight-strip PCR tubes (Axygen), and the reaction signals were generated by binding of SYBR green to double stranded DNA. qPCRs were carried out on an ABI Prism 7000 sequence detection system (Applied Biosystems USA).

For quantitative RT-PCR, 0.5 μg of total RNA extracted was used as template to produce cDNAs with random primers and oligo dT primers using ReverTra Ace® qPCR RT Master Mix with gDNA Remover (Toyobo).

16S rRNA gene and 16S rRNA copies of the *Ca. Methanoperedens* and the total archaea in HY soil in depth of 0 − 40 cm were quantified with the primer sets AAA641F/AAA834R and Arc915F/Arc1059R listed in Table S1, respectively. SYBR Premix Ex Taq Kit (Takara Bio Inc., Japan) was used to perform qPCR as described by Zhao et al (Zhao et al., 2011). Each qPCR mixture contains 12.5 μL SYBR qPCR mix (TOYOBO), 5 μL DNA, 100 nM of each primer, and double-distilled H_2O to a final volume of 25 μL. PCR was initiated at 95 °C of denaturation for 30 s and 35 cycles of amplification as follows: 95 °C at 10 s, 57 °C at 30 s, and 72 °C at 30 s. Fluorescence data were collected during elongation. Triplicated experiments were

performed. To estimate the copy numbers of the 16S rRNAs, standard curves were generated using 10-fold serially diluted PCR product with measured concentration as assayed using NanoDropND-100 Spectrophotometer (Gene Company) as templates.

Metagenomic assembly and contig binning of *Ca. Methanoperedens*

The raw sequencing reads of three enriched samples were processed with MetaWRAP v1.2.2 (Uritskiy et al., 2018), and the integrated pipeline for metagenomic data analysis. Raw paired-end reads were filtered and quality-controlled firstly using read_qc module in metaWRAP (Uritskiy et al., 2018). Clean reads generated for each sample were assembled individually using MEGAHIT v1.1.3 (Li et al., 2015) with default parameters, and short contigs (<1,000 bp) were removed. Multiple contig binning methods (CONCOCT v1.0.0 (Alneberg et al., 2014), MetaBAT2 v2.12.1 (Kang et al., 2015) and MaxBin2 v2.2.6 (Wu et al., 2016)) applied in binning module of MetaWRAP (Uritskiy et al., 2018) were used to recover the initial metagenome-assembled genomes (MAGs). Then, three MAG sets were merged and refined into a final MAG set for each sample using the bin_refinement module in metaWRAP (Uritskiy et al., 2018). Taxonomy prediction of the selected MAGs was classified using GTDB-Tk v1.0.2 (Parks et al., 2020) (classify_wf workflow, default parameter). Functional annotation was predicted using Prokka v1.13 (Seemann, 2014) and KofamKOALA (Aramaki et al., 2020).

Comparative genome analysis

Comparative genome analysis of MAG Fe_bin.173 and the reference MAGs of *M. nitroreducens*, *M. nitroreducens* BLZ1, *M. ferrireducens* and *M. manganireducens*

were conducted with OrthoFinder v2.4.0 (Emms and Kelly, 2015) using default parameters. Homologous proteins across all MAGs and unique proteins in Fe_bin.173 MAG was extracted for Venn plot using webtools (http://bioinformatics.psb.ugent.be/webtools/Venn/) and genetic diversity analysis.

Phylogenomic analysis

Phylogenomic relationship of the three Methanoperedenaceae MAGs enriched from ferric citrate and 43 reference genomes was inferred based on the concatenated set of 122 archaea-specific marker proteins using GTDB-Tk v1.0.2 (Parks et al., 2020). The maker proteins were identified and aligned individually using the identify and align module in GTDB-Tk with default settings. The maximum-likelihood phylogenomic tree was then constructed with IQ-TREE v2.0.3 (Minh et al., 2020) (using parameters: -bb 1000 -m TEST -nt AUTO), and visualized and edited using iToL v5 (Letunic and Bork, 2019). The whole-genome based average nucleotide identity (gANI) were estimated using the web tools ANI (https://ani.jgi-psf.org/html/calc.php) (Konstantinidis and Tiedje, 2005) and the average amino acid identity (AAI) was performed using the web tool AAI calculator (https://enve-omics.ce.gatech.edu/aai/) (Rodriguez-R and Konstantinidis, 2014).

Construction of the Methanoperedenaceae 16S rRNA tree

The Methanoperedenaceae 16S rRNA gene sequences in a consensus length 1007 bp that were amplified from the wetland soil were aligned with the relative 16S rRNAs retrieved from the SILVA database using ClustW software. The phylogenetic tree was constructed using neighbor-joining algorithm with software MEGA 6.0. Support values

were determined using 1000 nonparametric bootstrapping.

Data availability

All data supporting the findings of this study are available in this paper and the Supplementary Information. The Illumina sequencing data of archaeal 16S rRNA gene V4 and V5 regions are deposited at the NCBI Sequence Read Archive under accession number PRJNA720266; the sequencing data of 16S rRNA amplicons are under the NCBI GenBank accession MW674655, MW737675 − MW737676, MW737679 − MW757685. The data of the three assembled metagenomes of *Ca. Methanoperedens* sp. Fe_bin.166, *Ca. Methanoperedens* sp. Fe_bin.165 and *Ca. Methanoperedens* sp. Fe_bin.173 are deposited in NCBI database under accession numbers of JAGFNB000000000, JAGFNC000000000 and JAGFND000000000, respectively.

Acknowledgments

This work is supported by National Natural Science Foundation of China (Grant nos. 91751203 and 32070061).

References

Ajwa, H.A., and Tabatabai, M.A. (1993) Comparison of some methods for determination of sulfate in soils. *Commun Soil Sci Plan* **24**: 1817-1832.

Alneberg, J., Bjarnason, B.S., de Bruijn, I., Schirmer, M., Quick, J., Ijaz, U.Z. et al. (2014) Binning metagenomic contigs by coverage and composition. *Nat Methods* **11**: 1144-1146.

Aramaki, T., Blanc-Mathieu, R., Endo, H., Ohkubo, K., Kanehisa, M., Goto, S., and Ogata, H. (2020) KofamKOALA: KEGG Ortholog assignment based on profile HMM and adaptive score threshold. *Bioinformatics* **36**: 2251-2252.

476 Bonneville, S., Behrends, T., and Van Cappellen, P. (2009) Solubility and dissimilatory
477 reduction kinetics of iron(III) oxyhydroxides: A linear free energy relationship.
478 *Geochim Cosmochim Ac* **73**: 5273-5282.
479 Cai, C., Leu, A.O., Xie, G.J., Guo, J., Feng, Y., Zhao, J.X. et al. (2018) A
480 methanotrophic archaeon couples anaerobic oxidation of methane to Fe(III)
481 reduction. *ISME J* **12**: 1929-1939.
482 Caporaso, J.G., Kuczynski, J., Stombaugh, J., Bittinger, K., Bushman, F.D., Costello,
483 E.K. et al. (2010) QIIME allows analysis of high-throughput community sequencing
484 data. *Nat Methods* **7**: 335-336.
485 Cooper, C.R., Daugherty, A.J., Tachdjian, S., Blum, P.H., and Kelly, R.M. (2009) Role
486 of vapBC toxin-antitoxin loci in the thermal stress response of *Sulfolobus*
487 *solfataricus*. *Biochem Soc Trans* **37**: 123-126.
488 Ding, J., Fu, L., Ding, Z.W., Lu, Y.Z., Cheng, S.H., and Zeng, R.J. (2016) Experimental
489 evaluation of the metabolic reversibility of ANME-2d between anaerobic methane
490 oxidation and methanogenesis. *Appl Microbiol Biot* **100**: 6481-6490.
491 Eichler, J. (2020) N-glycosylation in archaea-new roles for an ancient posttranslational
492 modification. *Mol Microbiol* **114**: 735-741.
493 Emms, D.M., and Kelly, S. (2015) OrthoFinder: solving fundamental biases in whole
494 genome comparisons dramatically improves orthogroup inference accuracy.
495 *Genome Biol* **16**:157.
496 Ettwig, K.F., Zhu, B.L., Speth, D., Keltjens, J.T., Jetten, M.S.M., and Kartal, B. (2016)
497 Archaea catalyze iron-dependent anaerobic oxidation of methane. *Proc Natl Acad*
498 *Sci U S A* **113**: 12792-12796.
499 Gupta, V., Smemo, K.A., Yavitt, J.B., Fowle, D., Branfireun, B., and Basiliko, N. (2013)
500 Stable isotopes reveal widespread anaerobic methane oxidation across latitude and
501 peatland type. *Environ Sci Technol* **47**: 8273-8279.
502 Haroon, M.F., Hu, S.H., Shi, Y., Imelfort, M., Keller, J., Hugenholtz, P. et al. (2013)
503 Anaerobic oxidation of methane coupled to nitrate reduction in a novel archaeal
504 lineage. *Nature* **500**: 567-570.
505 He, Z.F., Zhang, Q.Y., Feng, Y.D., Luo, H.W., Pan, X.L., and Gadd, G.M. (2018)

Microbiological and environmental significance of metal-dependent anaerobic oxidation of methane. *Sci Total Environ* **610**: 759-768.

Hernsdorf, A.W., Amano, Y., Miyakawa, K., Ise, K., Suzuki, Y., Anantharaman, K. et al. (2017) Potential for microbial H_2 and metal transformations associated with novel bacteria and archaea in deep terrestrial subsurface sediments. *ISME J* **11**: 1915-1929.

Hu, S.H., Zeng, R.J., Burow, L.C., Lant, P., Keller, J., and Yuan, Z.G. (2009) Enrichment of denitrifying anaerobic methane oxidizing microorganisms. *Environ Microbiol Rep* **1**: 377-384.

Jin, H.J., Wu, J., Cheng, G.D., Tomoko, N., and Sun, G.Y. (1999) Methane emissions from wetlands on the Qinghai-Tibet Plateau. *Chinese Sci Bull* **44**: 2282-2286.

Kang, D.W.D., Froula, J., Egan, R., and Wang, Z. (2015) MetaBAT, an efficient tool for accurately reconstructing single genomes from complex microbial communities. *Peerj* **3** :e1165.

Kletzin, A., Heimerl, T., Flechsler, J., van Niftrik, L., Rachel, R., and Klingl, A. (2015) Cytochromes *c* in Archaea: distribution, maturation, cell architecture, and the special case of *Ignicoccus hospitalis*. *Front Microbiol* 6: 439.

Konstantinidis, K.T., and Tiedje, J.M. (2005) Genomic insights that advance the species definition for prokaryotes. *Proc Natl Acad Sci U S A* **102**: 2567-2572.

Letunic, I., and Bork, P. (2019) Interactive Tree Of Life (iTOL) v4: recent updates and new developments. *Nucleic Acids Res* **47**: W256-W259.

Leu, A.O., Cai, C., McIlroy, S.J., Southam, G., Orphan, V.J., Yuan, Z.G. et al. (2020) Anaerobic methane oxidation coupled to manganese reduction by members of the Methanoperedenaceae. *ISME J* **14**: 1030-1041.

Li, D., Liu, C.M., Luo, R., Sadakane, K., and Lam, T.W. (2015) MEGAHIT: an ultra-fast single-node solution for large and complex metagenomics assembly via succinct de Bruijn graph. *Bioinformatics* **31**: 1674-1676.

Li, L.Y., Ren, M.F., Xu, Y.Q., Jin, C., Zhang, W.H., and Dong, X.Z. (2020) Enhanced glycosylation of an S-layer protein enables a psychrophilic methanogenic archaeon to adapt to elevated temperatures in abundant substrates. *FEBS Lett* **594**: 665-677.

Lu, Z.K., Wang, H., Zhang, A.L., and Tan, Y.S. (2016) The VapBC1 toxin-antitoxin complex from *Mycobacterium tuberculosis*: purification, crystallization and X-ray diffraction analysis. *Acta Crystallogr F Struct Biol Commun* **72**: 485-489.

McGlynn, S.E., Chadwick, G.L., Kempes, C.P., and Orphan, V.J. (2015) Single cell activity reveals direct electron transfer in methanotrophic consortia. *Nature* **526**: 531-U146.

Meulepas, R.J.W., Jagersma, C.G., Gieteling, J., Buisman, C.J.N., Stams, A.J.M., and Lens, P.N.L. (2009) Enrichment of anaerobic methanotrophs in sulfate-reducing membrane bioreactors. *Biotechnol Bioeng* **104**: 458-470.

Minh, B.Q., Schmidt, H.A., Chernomor, O., Schrempf, D., Woodhams, M.D., von Haeseler, A., and Lanfear, R. (2020) IQ-TREE 2: New models and efficient methods for phylogenetic inference in the genomic era. *Mol Biol Evol* **37**: 1530-1534.

Narihiro, T., and Sekiguchi, Y. (2011) Oligonucleotide primers, probes and molecular methods for the environmental monitoring of methanogenic archaea. *Microb Biotechnol* **4**: 585-602.

Parks, D.H., Chuvochina, M., Chaumeil, P.A., Rinke, C., Mussig, A.J., and Hugenholtz, P. (2020) A complete domain-to-species taxonomy for Bacteria and Archaea. *Nat Biotechnol* **38**: 1079-1086.

Rodriguez-R, L.M., and Konstantinidis, K.T. (2014) Bypassing cultivation to identify bacterial species. *Microbe Magazine* **9**: 111-118.

Romaniuk, K., Krucon, T., Decewicz, P., Gorecki, A., and Dziewit, L. (2017) Molecular characterization of the pA3J1 plasmid from the psychrotolerant Antarctic bacterium *Pseudomonas* sp ANT_J3. *Plasmid* **92**: 49-56.

Saunders, N.F.W., Ng, C., Raftery, M., Guilhaus, M., Goodchild, A., and Cavicchioli, R. (2006) Proteomic and computational analysis of secreted proteins with type 1 signal peptides from the antarctic archaeon *Methanococcoides burtonii*. *J Proteome Res* **5**: 2457-2464.

Seemann, T. (2014) Prokka: rapid prokaryotic genome annotation. *Bioinformatics* **30**: 2068-2069.

Segarra, K.E., Schubotz, F., Samarkin, V., Yoshinaga, M.Y., Hinrichs, K.U., and Joye,

S.B. (2015) High rates of anaerobic methane oxidation in freshwater wetlands reduce potential atmospheric methane emissions. *Nat Commun* **6**: 7477.

Shi, L.D., Guo, T., Lv, P.L., Niu, Z.F., Zhou, Y.J., Tang, X.J. et al. (2020) Coupled anaerobic methane oxidation and reductive arsenic mobilization in wetland soils. *Nat Geoscience* **13**: 799-808.

Shukla, H.D., and DasSarma, S. (2004) Complexity of gas vesicle biogenesis in Halobacterium sp strain NRC-1: Identification of five new proteins. *J Bacteriol* **186**: 3182-3186.

Timmers, P.H.A., Suarez-Zuluaga, D.A., van Rossem, M., Diender, M., Stams, A.J.M., and Plugge, C.M. (2016) Anaerobic oxidation of methane associated with sulfate reduction in a natural freshwater gas source. *ISME J* **10**: 1400-1412.

Uritskiy, G.V., DiRuggiero, J., and Taylor, J. (2018) MetaWRAP-a flexible pipeline for genome-resolved metagenomic data analysis. *Microbiome* 6: 158.

Vaksmaa, A., Guerrero-Cruz, S., van Alen, T.A., Cremers, G., Ettwig, K.F., Luke, C., and Jetten, M.S.M. (2017) Enrichment of anaerobic nitrate-dependent methanotrophic 'Candidatus Methanoperedens nitroreducens' archaea from an Italian paddy field soil. *Appl Microbiol Biotechnol* **101**: 7075-7084.

Wang, Y.Y., Wang, H., He, J.S., and Feng, X.J. (2017) Iron-mediated soil carbon response to water-table decline in an alpine wetland. *Nat Commun* **8**: 15972.

Wegener, G., Krukenberg, V., Riedel, D., Tegetmeyer, H.E., and Boetius, A. (2015) Intercellular wiring enables electron transfer between methanotrophic archaea and bacteria. *Nature* **526**: 587-U315.

Wu, Y.W., Simmons, B.A., and Singer, S.W. (2016) MaxBin 2.0: an automated binning algorithm to recover genomes from multiple metagenomic datasets. *Bioinformatics* **32**: 605-607.

Xie, F., Ma, A.Z., Zhou, H.C., Liang, Y., Yin, J., Ma, K. et al. (2020) Niche differentiation of denitrifying anaerobic methane oxidizing bacteria and archaea leads to effective methane filtration in a Tibetan alpine wetland. *Environ Int* **140**: 11.

Yang, S.S., Lv, Y.X., Liu, X.P., Wang, Y.Z., Fan, Q.L., Yang, Z.F. et al. (2020) Genomic and enzymatic evidence of acetogenesis by anaerobic methanotrophic

archaea. *Nat Commun* **11**: 3941.

Zhang, C.Y., Liu, X.L., and Dong, X.Z. (2004) *Syntrophomonas curvata* sp nov., an anaerobe that degrades fatty acids in co-culture with methanogens. *Int J Syst Evol Microbiol* **54**: 969-973.

Zhang, G., Jiang, N., Liu, X., and Dong, X. (2008a) Methanogenesis from Methanol at Low Temperatures by a Novel Psychrophilic Methanogen, "*Methanolobus psychrophilus*" sp. nov., Prevalent in Zoige Wetland of the Tibetan Plateau. *Appl Environ Microbiol* **74**: 6114-6120.

Zhang, G.S., Tian, J.Q., Jiang, N., Guo, X.P., Wang, Y.F., and Dong, X.Z. (2008) Methanogen community in Zoige wetland of Tibetan plateau and phenotypic characterization of a dominant uncultured methanogen cluster ZC-I. *Environ Microbiol* **10**: 1850-1860.

Zhao, H.P., Van Ginkel, S., Tang, Y.N., Kang, D.W., Rittmann, B., and Krajmalnik-Brown, R. (2011) Interactions between perchlorate and nitrate reductions in the biofilm of a hydrogen-based membrane biofilm reactor. *Environ Sci Technol* **45**: 10155-10162.

Zhou, X.D., Xu, M.Z., Wang, Z.Y., Yu, B.F., and Shao, X.J. (2019) Responses of macroinvertebrate assemblages to environmental variations in the river-oxbow lake system of the Zoige wetland (Bai River, Qinghai-Tibet Plateau). *Sci Total Environ* **659**: 150-160.

Table and Figure legends

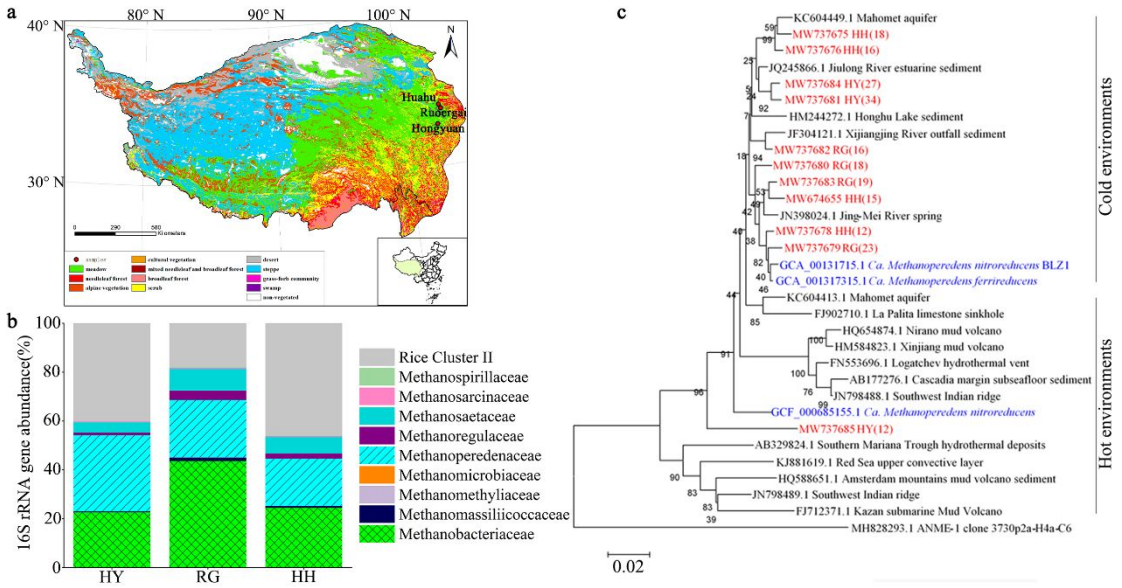

Figure 1. Geography location of the investigated Zoige wetland and the phylogenetic diversity of the inhabited *Ca. Methanoperedens* population. (a) The geography locations of the sampling sites of Hua-hu (HH), Ruo-er-gai (RG) and Hong-yuan (HY) at Zoige wetland are shown in the map. (b) The top 10 archaeal families were determined based on the relative abundances the 16S rRNA gene sequencing reads. (c) The phylogeny of the *Ca. Methanoperedens* archaea in Zoige wetland was analyzed based on the homology of 16S rRNA gene in a consensus length of 1 kb that were amplified using modified from the wetland soil. The phylogenetic tree was constructed using Neighbour-joining algorithms with MEGA6.0 and ANME-16S rRNA sequence was included as an outgroup. The tree topology was estimated by bootstraps based on 1,000 replications, and number at each branch node shows the percentage supported by

bootstraps. The *Ca. Methanoperedens*-specific sequences are shown in red letters, and reference sequences from NCBI nucleotide are in black and from the genome database are in blue. Prefixes represent 16S rRNA gene accession numbers and in parenthesis are clone numbers of each sequence. Bar, 2% sequence divergence.

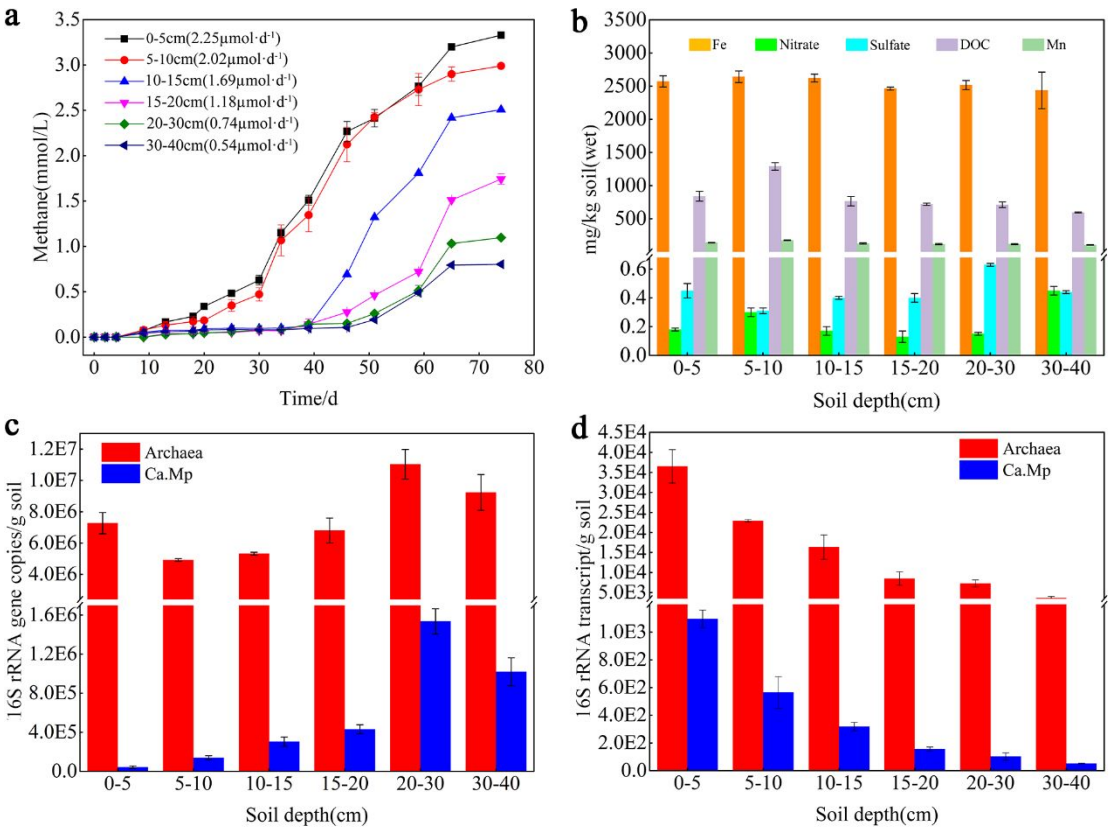

Figure 2. Cooccurrence of anaerobic oxidation of methane related environmental parameters and distribution of *Ca. Methanoperedens* in HY site of the cold Zoige wetland. (a) Methane emission rates were measured in the soil slurry prepared with different soil layers and incubated at 18°C. Methane was measured by GC during 70-day incubation. (b) Dissolved organic carbon (DOC), soluble nitrate (NO_3^-), soluble sulfate (SO_4^{2-}), soluble iron (Fe) and manganese (Mn) in various soil layers were measured using the methods described in the Experimental Procedures. (c) Using

quantitative PCR, the 16S rRNA gene copies of the total archaea (Archaea) and *Ca. Methanoperedens* (Ca. Mp) in the same six soil layers were quantified. (d) Using reverse transcription quantitative PCR, the 16S rRNA copies of the total archaea (Archaea) and *Ca. Methanoperedens* (Ca. Mp) in the same six soil layers were quantified. All the experiments were performed in triplicate, and the averages and standard deviations are shown.

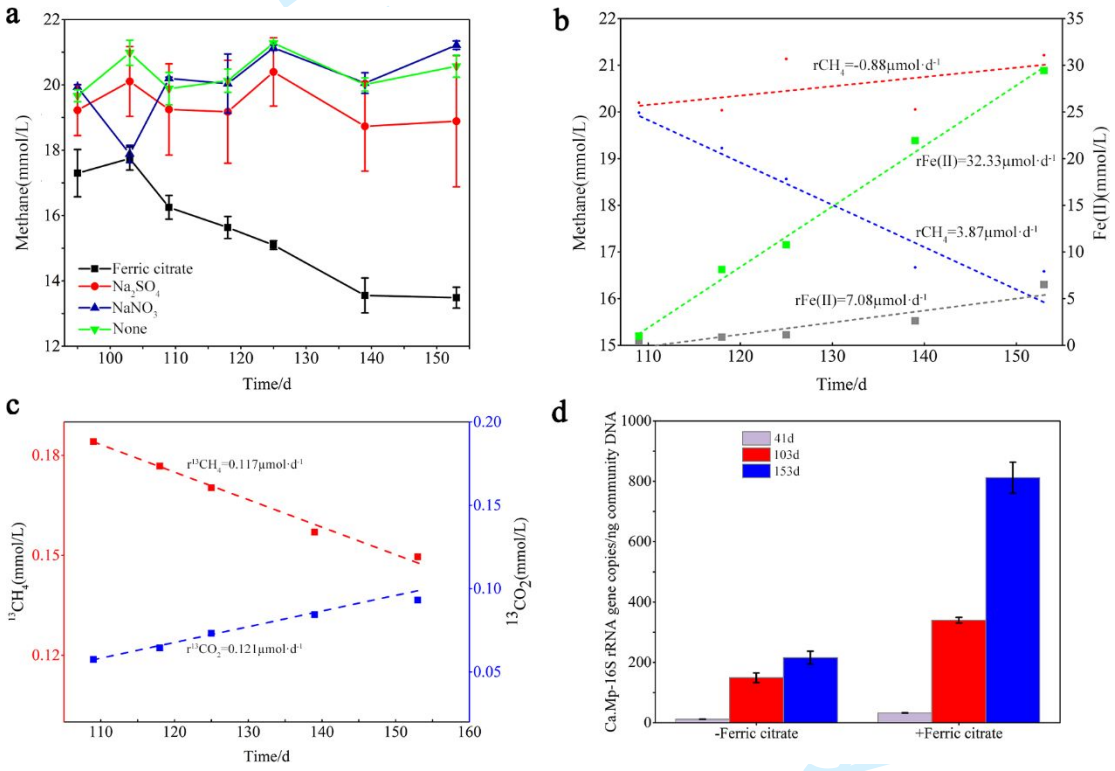

Figure 3. A lower temperature enrichment obtained from the Zoige wetland couples AOM to Fe (III) reduction. (a) CH_4 (0.1 MPa) was added to the soil enrichment and 20 mM of either ferric citrate, or Na_2SO_4, or $NaNO_3$ were amended in every two-week together with each 100 mM of ampicillin and kanamycin. Non-addition of electron acceptor was included as a control. Through GC measurement, methane degradation was determined until 95-day incubation at 18℃. (b) Methane consumption rates (rCH_4)

in the enrichments amended with ferric citrate (blue dot line) or not (red dot line) were computed; meanwhile, Fe(Ⅱ) accumulation rates (rFe(II)) were calibrated in AOM enrichments amended with Fe(III) (green dot line) or not (grey dot line). (c) $^{13}CH_4$ (0.2% total CH_4) was amended in the Fe (III) reduction coupled AOM enrichment at day 110 incubation, and then $^{13}CH_4$ consumption rate ($r^{13}CH_4$) and $^{13}CO_2$ accumulation rate ($r^{13}CO_2$) were measured. (d) Changes of the *Ca. Methanoperedens* 16S rRNA gene copies during incubation of Fe(III) reduction coupled AOM were assayed by qPCR using the primer pairs of AAA641F/ AAA834R. Triplicated experiments were performed, and the averages and standard deviations are shown.

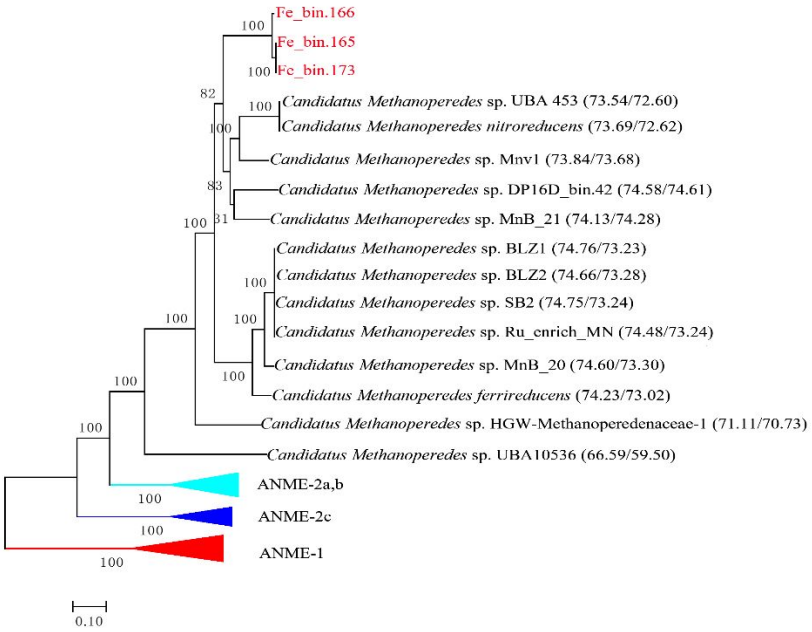

Figure 4. Phylogenomic analysis of the *Ca. Methanoperedens* retrieved from HY site of the Zoige wetland and the relatives. Phylogenomic relationship of the three *Ca. Methanoperedens* MAGs (red letters) from Zoige wetland and reference genomes was inferred based on the concatenated 122 archaeal marker proteins using GTDB-Tk v1.0.2. The maker proteins were identified and aligned individually using the identify

and align module in GTDB-Tk with default settings. The maximum-likelihood phylogenomic tree was constructed with IQ-TREE v2.0.3 using parameters: -bb 1000 -m TEST -nt AUTO, and visualized and edited using iToL v5. Bootstrap values were calculated from 1000 replicates and shown when bootstrap values >50. Scale bar indicate 0.1 amino acid substitutions per site. Inside the parenthesis are the whole-genome based average nucleotide identity (gANI/) and average amino acid identity (/gAAI) between Fe_bin.173 and other *Ca. Methanoperedens* deposited in the NCBI database.

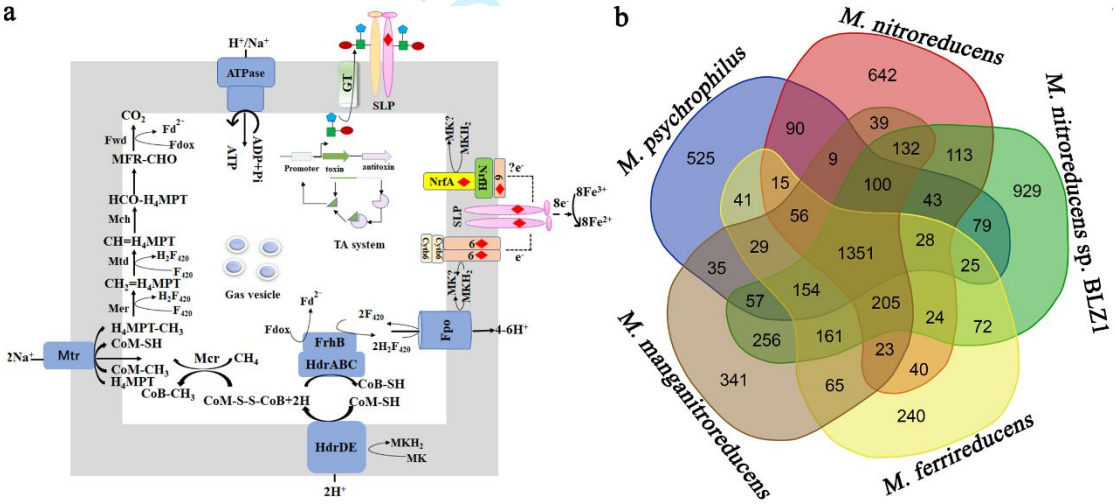

Figure 5. Metabolic construction of the putative Fe (III) reduction coupled AOM pathway (a) and the distinct genes in the *Ca. Methanoperedens psychrophilus* MAG (b). (a) Methane is oxidized via the "reverse methanogenesis" pathway, and the generated electrons are transferred to menaquinone pool (MK/MKH_2) via Fpo and Hdr complexes, which oxidize $F_{420}H_2$ and CoM-SH-CoB-SH, respectively. Reducing equivalents are then transferred to MHCs associated three types of membrane proteins: the NrfA-NrfH like protein complexes, the extracellular S-layer architecture protein

(SLP), and class III cytochrome *c* family (6 ♦), and then to reduce the Fe (III) oxides. Abbreviations of enzymes and co-factors: H_4MPT, tetrahydromethanopterin; MFR, methanofuran; Fwd, formylmethanofuran dehydrogenase; Ftr, formylmethanofuran-H_4MPT formyltransferase; Mch, methenyl-H_4MPT cyclohydrolase; Mtd, F_{420}-dependent methylene H_4 MPT dehydrogenase; Mer, F_{420}-dependent methylene-H_4MPT reductase; Mtr, Na^+-translocating methyl-H_4MPT:coenzyme M methyltransferase; Mcr, methyl-coenzyme M reductase; Fpo, $F_{420}H_2$ dehydrogenase; MK, menaquinone; CoB-SH, coenzyme B; CoM-SH, coenzyme M; Fd, ferredoxin; Hdr, heterodisulfide reductase; FrhB, F_{420}-reducing hydrogenase subunit B; Cytb, b-type cytochrome; NrfA and NrfH, nitrite reductase subunit A and H; ♦, heme and numbers are indicated. (b) The Venn diagram shows the shared and the distinct gene numbers among the four *Ca. Methanoperedens* spp. based on comparative genome analysis.